Generation of porosity in a hybrid organic-inorganic xerogel by chemical treatment

Bruno Boury,[a] Robert J. P. Corriu,*[a] Valérie Le Strat[a] and Pierre Delord[b]

[a] *Laboratoire de Chimie Moléculaire et Organisation du Solide (CNRS UMR 5637)*
[b] *Groupe de Dynamique des Phases Condensées (CNRS UMR 5581), Université Montpellier II, Place E. Bataillon, 34095 Montpellier cedex 5, France*

Received (in Strasbourg, France) 21st December 1998, Accepted 1st March 1999

A hybrid xerogel of 1,4-bis(trimethoxysilylethynyl)benzene was prepared by using a sol-gel process. Chemical treatment of this material was performed under mild conditions in order to remove the organic group using fluoride anion as a catalyst. Experimental procedures were carried out using different solvents, acidities and counter-cations in order to modify the nucleophilic power of F^-. Characterization of the residues was done by elemental analysis, spectroscopy (^{29}Si NMR), thermal analysis, pycnometry, surface area measurement and SAXS. The efficiency of the chemical treatment is related to the solvation of the F^- anion. It was possible to demonstrate that elimination of the organic part occurs at the same time as a reorganization of the silica network. This reorganization is the result of two competitive F^--catalyzed chemical reactions: a redistribution and a polycondensation process known in solution and which take place in the solid. These processes account for the textural characteristics of the final material and may efface the organization of the organic spacers in the hybrid xerogel. These results demonstrate the limitations of silica as a molecular imprinting material and open a new approach to porous silica with adjustable pore size.

Molecular imprinting, or footprint as originally proposed by Dickey,[1] is a great challenge for chemistry.[2] In many cases silica has been selected as a support.[3–5] On the other hand, preparation of micro- and mesoporous silica-based materials is also a rapidly expanding field of investigation with two targets: the access to a controlled monodispersed porosity and molecular imprinting. The organic templating of amorphous silica is not straightforward, but it can be achieved by different means as suggested and recently reviewed by Brinker *et al.*[6,7] In the cases of nanocomposites (non-covalently bonded organic group), removal of the organic groups used as templates is achieved by washing or by thermal treatment. Porous silicas have been obtained by removing various organic templates like dendrimers,[8] polymers,[9] micellar rods,[10,11] liquid crystals,[12] and more recently dopamine,[13] glucose and maltose.[14]

In the case of nanostructured hybrid solids (covalently bonded organic group), thermal oxidation at high temperature is generally used successfully to remove the organic moiety.[7] The general formula of these materials, $(O)_{1.5}Si{-}R{-}Si(O)_{1.5}$ or $RSi(O)_{1.5}$, allows a homogeneous distribution of the organic group within the material.[15–19] However, the ability to design the porosity with such materials is related to the organic group's volume fraction, the level of condensation of the silica network and the modification of the silica network (shrinkage, relaxation, sintering) during the thermal treatment. In order to test the limits and the possibilities of silica as a support in molecular imprinting, we have recently compared thermal elimination and a selective chemical elimination in the case of nanostructured hybrid xerogels of the general formula $(O)_{1.5}Si{-}C{\equiv}C{-}R{-}C{\equiv}C{-}Si(O)_{1.5}$.[20–23] They are prepared by hydrolysis of a molecular precursor (Scheme 1). The reproducibility of the starting hybrid xerogel's texture was achieved by controlling the kinetic parameters of the hydrolytic polycondensation leading to SiO_2 matrix formation. Different organic units with a precise size and a linear, planar or tetrahedral geometry were used as the molecular precursors. The $Si{-}C{\equiv}C$ group was used to obtain a selective cleavage of the $Si{-}C_{sp}$ bond under mild conditions ($MeOH{-}H_2O{-}2\%\ NH_4F$ at 60 °C). When a rigid organic group was used, in all cases it was possible to recover the molecular organic unit quantitatively.[21,22,24] Comparison with the thermal treatment (600 °C in dry air) is highly illustrative: the thermal treatment always leads to a very wide pore size distribution of ultramicropores ($d < 10$ Å) and mesopores ($20 < d < 200$ Å). On the other hand, the chemical treatment always provides a silica residue that exhibits a very narrow pore size distribution of mesopores (30 to 50 Å). However, the pore diameter is always significantly higher than the organic unit size. A tentative explanation of this discrep-

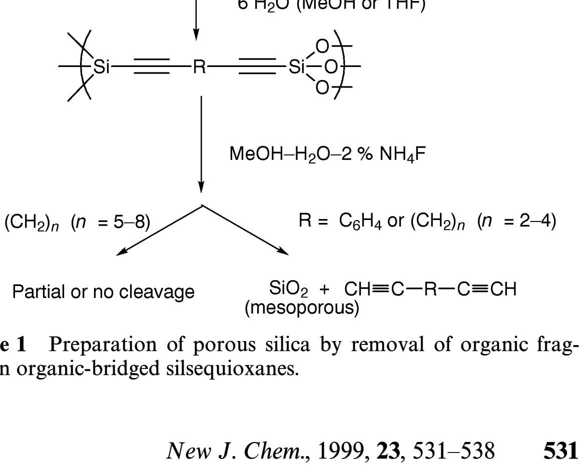

Scheme 1 Preparation of porous silica by removal of organic fragment in organic-bridged silsequioxanes.

ancy is based on two possible hypotheses, both having an experimental background.

(1) During the polycondensation step the organization of the organic group in the hybrid material can result in a structure where organic units are packed together. Evidence for such structuration is supported by the observation of reactions induced in the solid: the electrochemically and chemically induced polymerization of thiophene units in $(O)_{1.5}Si—(C_4H_4S)—Si(O)_{1.5}$[20] and the thermal crosslinking reaction of acetylenic units in $(O)_{1.5}Si—C{\equiv}C—C{\equiv}C—Si(O)_{1.5}$.[25] Therefore, the elimination of the organic groups during the chemical treatment might result in the formation of pores larger than the size of a single organic group because of a short-range organization in the solid.

(2) A chemically induced reorganization of the silica network, catalyzed by F^- anion, certainly occurs during the chemical treatment. The fluoride anion is known to catalyze cleavage of the $Si—C_{sp}$ bond but it was also found to promote activation of the Si—O bond.[26] Thus, the presence of F^- in the mixture could induce a reorganization of the Si—O—Si network under the conditions used for the chemical treatment of the hybrid material. This mechanism is similar to the nucleophilic-catalyzed redistribution induced by activation at silicon.[27–30]

In order to point out the relative influence of these two parameters we have investigated the behavior of a given hybrid material towards chemical treatment under different experimental conditions. The latter were chosen to change the nucleophilic power of F^-, and thus the kinetics of both the $Si—C_{sp}$ cleavage and the possible reorganization of the silica network (Scheme 2).

In this paper, we wish to report how silicas of various porosities are obtained after chemical treatment of a single hybrid xerogel $(O)_{1.5}Si—C{\equiv}C—(C_6H_4)—C{\equiv}C—Si(O)_{1.5}$.

Results

Preparation of the xerogel

Precursor **1**, containing a 1,4-bisethynylphenylene unit as spacer, was prepared following the synthesis pathway previously reported.[21,22] Hydrolysis of **1** was performed under mild conditions using a solution of **1** in THF and by adding a stoichiometric amount of deionized water (pH = 6) at room temperature in the *absence of any catalyst.* Polycondensation is ideally represented by eqn. (1). It led to gelation within 5 min and the resulting gel was allowed to age for 1 week at room temperature by further condensation. The gel was then powdered, washed with solvents and dried under vacuum for 24 h at 100 °C, giving the xerogel $\mathbf{H_1}$.

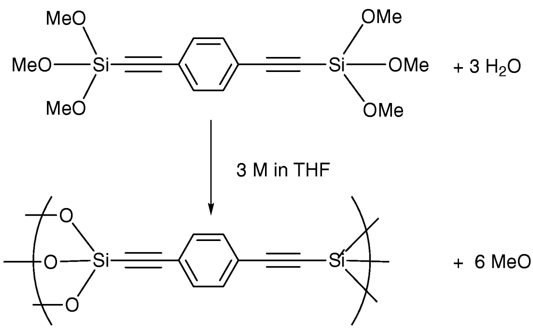

(1)

Chemical treatment of the xerogel H_1

The Si—C bond in the Si—C≡C group can be cleaved under mild conditions. This reaction is a well-documented process in organosilicon chemistry.[31–34] It corresponds to the reversible coordination of F^- at the silicon atom, leading to a pentacoordinated center in which the negative charge is delocalized onto the substituents bound to silicon. In the second step, the nucleophilic attack of H_2O cleaves the $Si—C_{sp}$ bond forming the corresponding acetylenic and silanol compounds. When the process is applied to the whole material, it corresponds ideally to eqn. (2). In this case, the Si—OH functions are expected to polycondense either with each other or with the residual Si—OMe groups left after polycondensation.

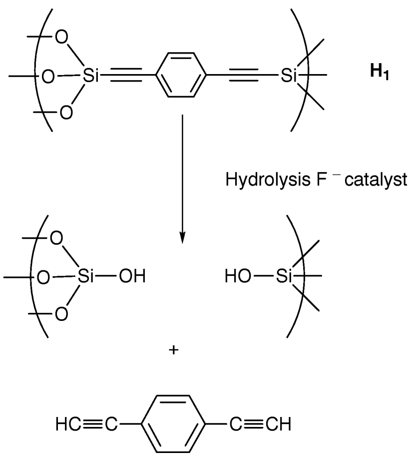

(2)

The different chemical treatments were performed on the same batch of xerogel using the experimental conditions presented in Scheme 2. After treatment, the solid residue was filtered, washed and dried in order to separate the soluble organic byproduct.

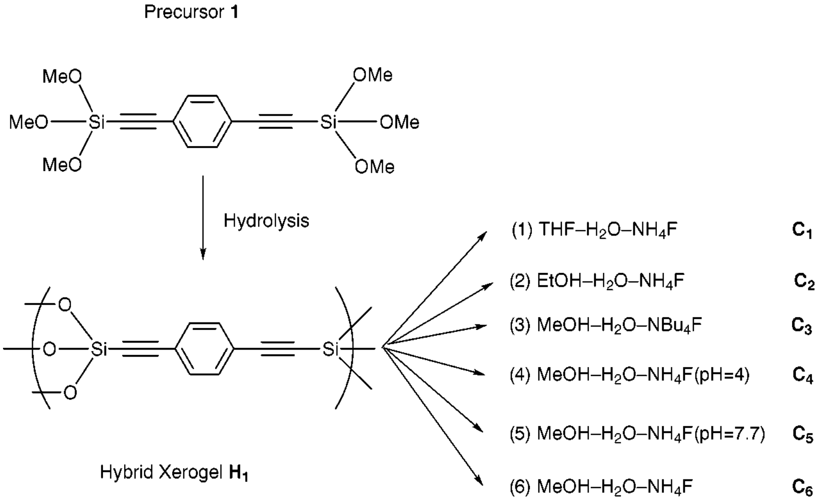

Scheme 2 Modification of the pore size of a porous silica prepared by mild removal of the organic group of a 1,4-bisethynylphenyl-bridged silsequioxanes.

Characterization of materials $\mathbf{C_{1-6}}$

Elemental analyses. The residues were initially analyzed by elemental analysis to evaluate the efficiency of the chemical treatment (Table 1). The low carbon content in materials $\mathbf{C_{2-6}}$ is consistent with a quantitative elimination of the organic spacer. The amount of residual spacer can be evaluated at 2 to 3%. For $\mathbf{C_1}$, the high level of carbon content indicates the persistence of almost 50% of the organic spacer.

Thermogravimetric analysis. These analyses were performed between 50 and 1000 °C in a flow of dry air in order to confirm the elemental analyses (Table 1). For the pure hybrid xerogel $\mathbf{H_1}$ and also for the residues obtained after chemical treatment of $\mathbf{C_{1-6}}$, weight loss occurred in two steps: a first limited weight loss between 50 and 250 °C corresponds to the elimination of absorbed residues and water formed by polycondensation of residual Si—OH. A second weight loss between 300 and 800 °C arises mainly from the formation of carbon dioxide and monoxide and water produced by the oxidation of the organic unit and condensation between resulting Si—OH groups. The latter weight loss is representative of the presence of the organic group in the material and therefore, this analysis was used to evaluate the level of carbon residue in $\mathbf{C_{1-6}}$. For the starting material $\mathbf{H_1}$, the weight losses are respectively equal to 2–3 and 43%, that is to say a total weight loss of 46%. The weight losses observed are 3 to 6% for $\mathbf{C_{2-6}}$ and 39.9% for $\mathbf{C_1}$; this confirms that the organic spacers were quantitatively removed from $\mathbf{H_1}$ using conditions 2 to 6 while condition 1 leaves 50% of the organic spacer in $\mathbf{C_1}$.

^{29}Si CP MAS NMR. To evaluate the local environment of the silicon atom in these xerogels, CP MAS (cross polarization magic angle spinning) is a convenient NMR sequence for solid state analysis. However, since the intensity of the signal is closely dependent on both the distance to and the number of hydrogen atoms in the environment of the silicon atoms, the peak intensity does not accurately represent the population in the sample. The signals observed for the starting hybrid xerogel $\mathbf{H_1}$ were characteristic of silicon atoms attached to three oxygen atoms and one C_{sp} atom: T^1, C—*Si*(OH)$_2$(OSi) at −79 ppm; T^2, C—*Si*(OH)(OSi)$_2$ at −87 ppm and T^3, C—*Si*(OSi)$_3$ at −96 ppm (spectra of $\mathbf{H_1}$ and $\mathbf{C_4}$ are given as examples in Fig. 1).[21,23,35] No signal corresponding to Q^n units was observed and this unambiguously indicates that cleavage of the Si—C_{sp} bond during the polycondensation step does not occur. Because of the presence of an important T^2 signal and in the absence of quantitative measurement, the structure of the hybrid network can be approximately described as siloxane chains with bridging units and with an average of one uncondensed OH or OMe group per silicon atom.

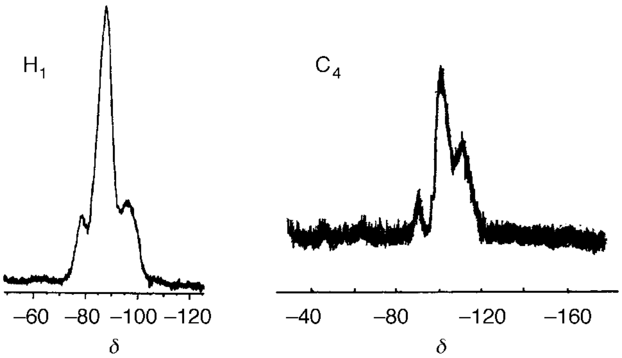

Fig. 1 ^{29}Si CP MAS NMR spectra of $\mathbf{H_1}$ and $\mathbf{C_4}$.

After chemical treatment of $\mathbf{C_1}$, the main signals observed are at −100 and −110 ppm, corresponding respectively to Q^3 units [Si(OR)$_1$(OSi)$_3$ with R = H or CH$_3$] and Q^4 units [Si(OSi)$_4$]. Since the chemical cleavage is not complete, the signal at −91 ppm can be attributed to the simultaneous presence of Q^2 units [Si(OR)$_2$(OSi)$_2$ with R = H or CH$_3$] and residual T^3 units [C—Si(OR)(OSi)$_3$ with R = H or CH$_3$] arising from remaining silicon atoms linked to an organic spacer. In the case of $\mathbf{C_{2-6}}$, because of their low carbon content, the absence of T^n signal can be assumed and signals at −91, −100 and −110 ppm can be attributed respectively to Q^2, Q^3 and Q^4 units, corresponding to the hydrolysis of all the Si—C_{sp} bonds. Despite their qualitative aspect, comparison of these results can be attempted due to the similarity of the materials. For $\mathbf{C_3}$ and $\mathbf{C_5}$ a high level of condensation is apparently obtained since only signals for Q^3 and Q^4 units are observed. By comparison, treatment with conditions 2 and 4 leads to lower degrees of polycondensation than in cases 3, 5 and 6. Signals due to Q^2 units are observed for $\mathbf{C_2}$ and $\mathbf{C_4}$.

Nitrogen adsorption porosimetry. This analysis was selected to evaluate the specific surface area and the average pore size of these materials (Table 2). A 35-point adsorption/desorption isotherm plot measurement was used.[36,37] The specific surface area was evaluated using the BET equation, which is reliable when using mesoporous materials. The pore size distribution was given by the BJH method, calculated on the desorption isotherm branch.[38] A type IV isotherm adsorption/desorption plot was observed with a type H1 hysteresis loop (type A in the de Boer classification), corresponding to a mesoporous material with a low level of micropores (the isotherm of $\mathbf{C_4}$ is given as an example in Fig. 2). The hysteresis loop shape suggests the presence of regular cylindrical or ink-bottle pores. For all the materials, chemical treatment led to an increase of the specific surface area. Starting with a nonporous material (< 10 m^2 g^{-1}), the resulting silicas present a surface area of at least 180 m^2 g^{-1}, even when the chemical treatment does not remove the organic spacer efficiently as in condition 1. The BJH [dV/dLog(D)] curve shows a rather broad pore size distribution (±40 Å) centered at different values for the different silica; this curve for $\mathbf{C_4}$ is given as an example in Fig. 3. The specific surface area of these materials, like the pore size distribution, is clearly related to the experimental conditions used for the chemical treatment, varying from 655 m^2 g^{-1} for $\mathbf{C_6}$ to 180 m^2 g^{-1} for $\mathbf{C_3}$. The pore sizes are, in all cases, much higher than those estimated by molecular simulation using the cerius2 modelization program provided by MSI. This simulation indicates a Si···Si distance of 11.4 Å in the starting xerogel and O···O distance of 8.2 Å between the silanol groups formed by hydrolysis (Scheme 3).

Helium pycnometry. The density of the materials was determined by a pycnometry measurement with helium. The value of the density is 1.38 for the starting hybrid xerogel $\mathbf{H_1}$. Using this value, an estimation of the average volume occupied by each precursor molecule can be made. V_a, the average volume

Table 1 Elemental analysis and weight loss during thermal treatment of $\mathbf{C_{1-6}}$

	$\mathbf{H_1}$	$\mathbf{C_1}$	$\mathbf{C_2}$	$\mathbf{C_3}$	$\mathbf{C_4}$	$\mathbf{C_5}$	$\mathbf{C_6}$
Carbon content[a]	52.61	27.90	2.03	3.02	2.52	2.28	7.4
Weight loss upon calcination[b]	43.3	39.9	3.3	3.3	4.4	4.3	5.7

[a] Determined by elemental analysis. [b] TG analysis, 2nd peak weight loss.

Table 2 Nitrogen adsorption porosimetry surface analysis of $\mathbf{C}_{1-6}$

	$\mathbf{H}_1$	$\mathbf{C}_1$	$\mathbf{C}_2$	$\mathbf{C}_3$	$\mathbf{C}_4$	$\mathbf{C}_5$	$\mathbf{C}_6$
Density/g cm^{-3} [a]	1.38	1.55	2.04	2.09	2.04	2.06	2.08
Specific surface area/m^2 g^{-1} [b]	<10	255	590	180	300	260	655
Average pore radius/Å [b]	—	40	30	65	50	50	50

[a] Pycnometry measurement at 25 °C under 760 mm of Hg. [b] Measured by nitrogen porosimetry.

occupied by one unit, is equal to $(dN/\mathrm{MM})^{-1}$, where d is the hybrid xerogel's density, MM is the molecular weight for $-(\mathrm{O}_{1.5}\mathrm{Si}-\mathrm{C}\equiv\mathrm{C}-\mathrm{C}_6\mathrm{H}_4-\mathrm{C}\equiv\mathrm{C}-\mathrm{SiO}_{1.5})-$, N is Avogadro's number. The corresponding experimental value, $V_a = 2.74 \times 10^{-22}$ cm^3, is greater than the 1.7×10^{-22} cm^3 calculated by molecular simulation. Using cerius2, a model of the energy-minimized molecule was drawn, allowing an estimation of the distances between oxygen, silicon or hydrogen atoms. The volume occupied by the organic moiety was calculated assuming that the unit occupies a void with a cylindrical shape. This result indicates that the organic groups are not closely packed together in the hybrid xerogel. Using the experimental value it is also possible to estimate the expected density of the silica formed by elimination of the organic group *in the absence of any other transformation.* This calculated value of 0.35 is far from the experimental values of 2.04 to 2.09 measured for $\mathbf{C}_{2-6}$, which are close to the density of a silica gel obtained by sol-gel polycondensation of TMOS. The presence of a high level of residual organic groups in $\mathbf{C}_1$ accounts for the low density of 1.55 in this case, close to the starting one of $\mathbf{H}_1$.

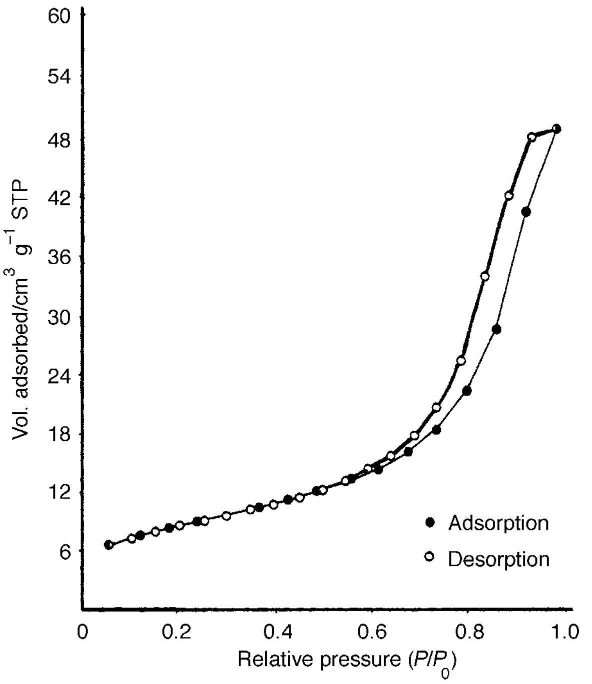

Fig. 2 Nitrogen adsorption/desorption isotherm plot of the hybrid xerogel $\mathbf{C}_4$.

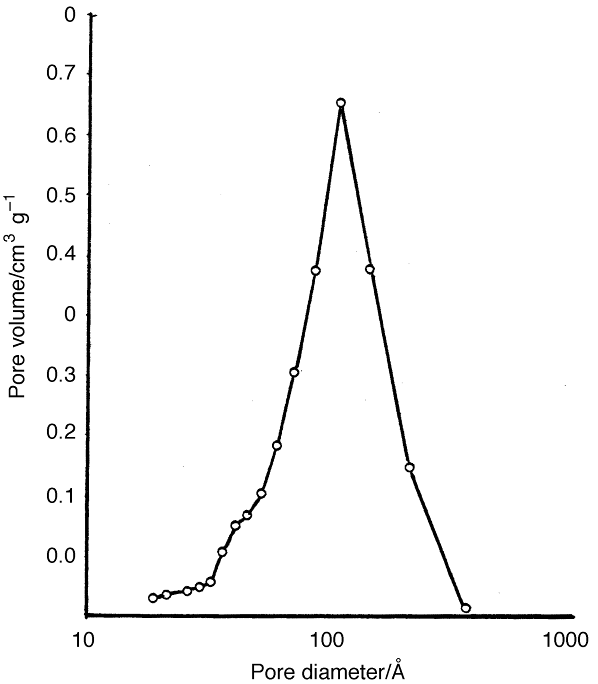

Fig. 3 BJH plot on the isotherm desorption branch of treated hybrid xerogel $\mathbf{C}_4$.

Small-angle X-ray scattering (SAXS). This technique is sensitive to the fluctuations of electronic density in the medium.[39,40] We have already reported the characterization of the porosity of hybrid xerogel $\mathbf{H}_1$, the small-angle scattering intensity decreases continuously between 2×10^{-3} and 1×10 Å^{-1}. A power law, between $q^{-2.5}$ and q^{-3}, represents correctly the intensity comportment between 5×10^{-3} and 1×10^{-1} Å^{-1} and fractal behavior might be assumed. We focus here on the related materials $\mathbf{C}_{1-6}$ prepared by chemical treatment (the curve for $\mathbf{C}_4$ is given as an example in Fig. 4). For the mesoporous silicas $\mathbf{C}_{2-6}$ obtained by chemical treatment of $\mathbf{H}_1$, a q^{-4} slope of the spectrum was measured in the Porod region between 0.08 Å $< q <$ 0.2 Å, indicating in all cases *a smooth surface of the silica phase*, which corresponds to a Porod behavior. For $\mathbf{C}_1$, this Porod behavior cannot be measured and the transition between the solid phase and the gas phase is certainly disturbed by the remaining organic groups.[40]

For the other materials, the asymptotic Porod behavior allows us to determine two parameters, K and Q, respectively Porod's limit and invariant.[41] According to the hypothesis of a porous material, we used the solid phase density ρ_s and volume fraction φ_s, and the gaseous phase volume fraction φ_p

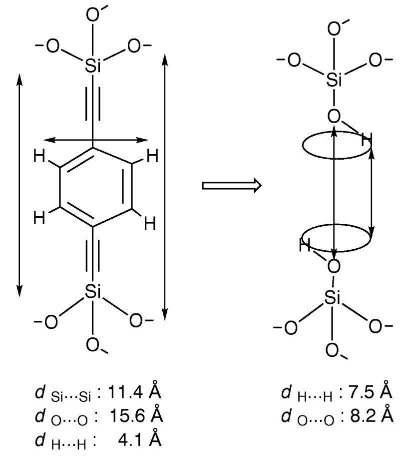

Scheme 3 Calculated distances in precursor **1**.

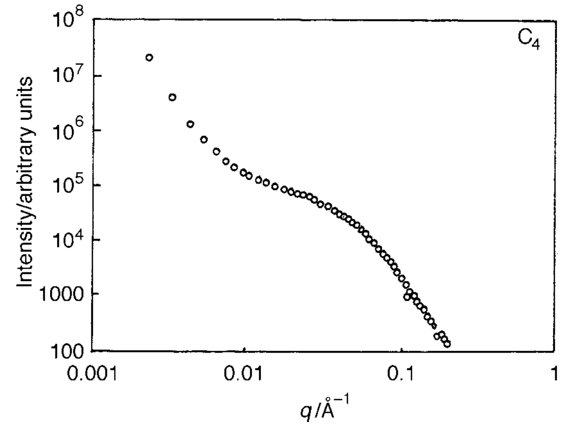

Fig. 4 SAXS measurement. Intensity *vs.* scattering vector *q* (log scale) for $\mathbf{C_4}$.

(φ_p being equal to zero) in order to calculate $\bar{l}$ from eqn. (3) and ultimately the parameters $\bar{l}_s$, $\bar{l}_p$ with eqn. (4, 5):

$$\bar{l} = AQ(\pi K)^{-1} \tag{3}$$

$$\bar{l}^{-1} = \bar{l}_s^{-1} + \bar{l}_p^{-1} \tag{4}$$

$$\bar{l} = \varphi_p \bar{l}_s = \bar{l}_p \varphi_s \tag{5}$$

$\bar{l}_s$ and $\bar{l}_p$ are the average cut lengths respectively in the solid and in the gas. Using these parameters, the specific surface area S_p can be calculated using eqn. (6):

$$S_p = 10^4 \pi K \varphi_p (Q\rho_s)^{-1} \tag{6}$$

The determination of φ_s generally requires monoliths like those obtained for aerogels. However, in the present case the porosimetry analysis allows the porous volume and consequently the solid volume to be determined, considering that all the pores are accessible.

Thus, φ_p and φ_s are taken from the porosimetry measurements and used for the calculation of $\bar{l}$, $\bar{l}_s$, and S_p. A good agreement between the specific surface area determined by porosimetry and S_p determined by SAXS is a test to verify the compatibility of the two methods. Similarly, $\bar{l}_p$ can be assimilated and is expected to be identical to the average pore radius determined by porosimetry (Table 3).

For $\mathbf{C_2}$ and $\mathbf{C_3}$, we find a good agreement between S_p determined by SAXS and the specific surface area measured by porosimetry. Similarly the average pore diameter is close to the value of $\bar{l}_p$. Therefore, this agreement between the two methods indicates the absence of closed porosity in these cases. For $\mathbf{C_4}$ and $\mathbf{C_5}$, S_p and $\bar{l}_p$ are different from their corresponding values determined by porosimetry, respectively the specific surface area and the pore radius. This discrepancy arises probably from the presence of a closed porosity measured by SAXS but not accessible to the porosimetry measurement. The closed porosity is rather important since it represents more than 30% of the total surface area determined by SAXS.

Discussion

Initially, the Si—C≡C group was chosen to link the phenylene group to the silica network because of the possibility to cleave the Si—C_{sp} bond by F^--catalyzed hydrolysis. The present results provide some elements for a better understanding of the chemistry occuring in the solid during the chemical treatment. At present it appears that the chemistry is rather complex but we can distinguish three main processes.

Table 3 Determination of S_p, $\bar{l}_p$ and $\bar{l}_s$ from SAXS analysis of $\mathbf{C_{2-5}}$

	$\mathbf{C_2}$	$\mathbf{C_3}$	$\mathbf{C_4}$	$\mathbf{C_5}$
S_p/m^2 g^{-1}	614	177	399	345
$\bar{l}_p$/Å	32	108	49	56
$\bar{l}_s$/Å	61	128	75	74

The first point is the efficiency of the chemical treatment to achieve complete cleavage of the Si—C_{sp} bond. This is apparently related to the nature of the solvent but is independent of both the pH and the associated cation (K^+ or NH_4^+) as demonstrated by experiments **2** to **6** in which carbon-free siliceous residues are obtained in all cases. From this point of view THF, methanol and ethanol are all polar solvents that easily solubilize the precursor and the organic fragment. Therefore, the lower efficiency observed when using THF is not a lack of affinity of the solvent for the material but is more probably due to a lower nucleophilic power of the fluoride anion in THF than in alcohols.

The second point is the polycondensation of the Si—OR (R = H or CH_3) group as demonstrated by the NMR data. Instead of the Q^1, Q^2 and Q^3 units expected for the hydrolysis of the T^1, T^2 and T^3 units in $\mathbf{H_1}$, we found no Q^1 units, only some Q^2 units, and mainly Q^3 and Q^4 units. This polycondensation can be promoted by the fluoride anion known to activate the Si—O bond.[26] However, other experimental conditions are determinant, for example a higher degree of polycondensation is favored by high pH and methanol as a solvent while the nature of the counter-cation associated with F^- has apparently no effect. This polycondensation requires a movement of the silica units formed by hydrolysis, as depicted in Scheme 4.

The third process that has to be considered is the reorganization of the silica network by a redistribution of the Si—O bonds between the different units. Such a process, like the polycondensation process, is catalyzed by fluoride anion and depicted in Scheme 5. This type of redistribution is well-known for homogeneous solutions or mixtures of functionalized silanes.

The comparison between measured and calculated density is very illustrative: in the absence of any other chemical reactions the expected density after Si—C_{sp} hydrolysis is very low (0.35), in great contrast with the experimental result (2.06 ± 0.03). Thus, the Si—C_{sp} cleavage should lead to a very light silica network due to the important voids left by the elimination of the organic groups. Therefore, the texture of the silica residue results from the sum of these three processes as depicted in Scheme 6.

The collapse of this structure and the percolation of the voids occur by polycondensation and reorganization of the silica units and leads to structure coarsening. Therefore, irrespective of the organization of the organic group in the

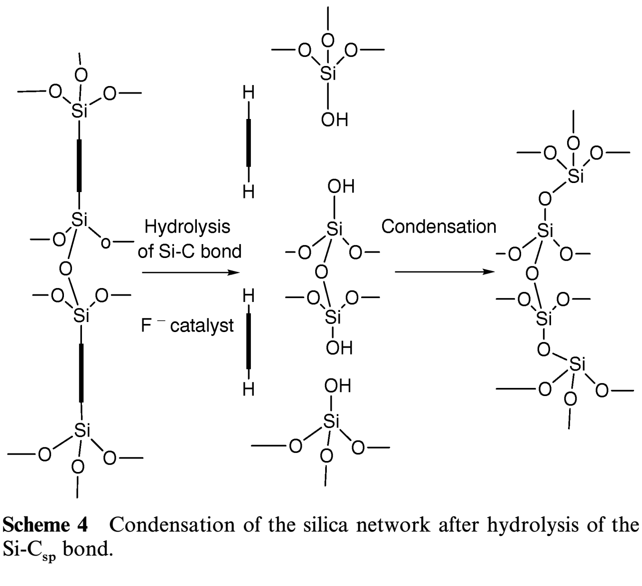

Scheme 4 Condensation of the silica network after hydrolysis of the Si-C_{sp} bond.

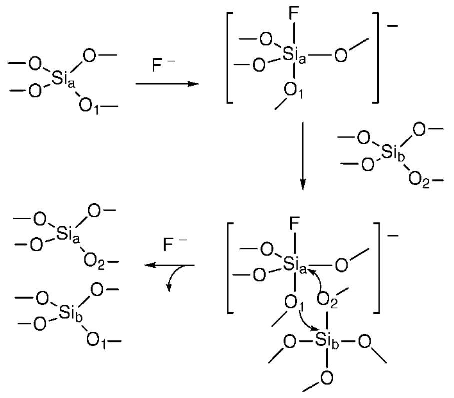

Scheme 5 F$^-$-catalyzed redistribution of the Si-O bonds of the silica network.

material, the information related to the size of the precursor is completely erased from the silica network by these processes. Finally, the specific surface area can vary from 180 m^2 g^{-1} in $\mathbf{C_3}$ to 655 m^2 g^{-1} in $\mathbf{C_6}$ and the average pore radius can vary from 30 Å in $\mathbf{C_2}$ to 65 Å in $\mathbf{C_3}$. The formation of this texture occurs with closed porosity for $\mathbf{C_{4,5}}$ or without it for $\mathbf{C_{2,3}}$. The influence of parameters like the nature of the solvent or the acidity is determinant on the texture of such materials as demonstrated by the polycondensation of silica precursors (TMOS or TEOS).[42] This evolution of the silica network seems bound to happen but we note that the pore size distribution is rather narrow and completely different from the evolution occurring under thermal treatment where a microporous silica is recovered.[21,22] From this point of view, the thermal treatment appears more appropriate for a molecular imprint in the silica, meanwhile the pore size distribution is rather broad. On the other hand, the chemical treatment described here is another method that can be used for a different aim since it offers the possibility to design the porosity of an oxide by chemical transformation of a hybrid material. Starting with the same hybrid xerogel, siliceous residues with different porosities can be obtained, depending on the experimental conditions.

Conclusion

Removal of the organic moiety from an organic–inorganic hybrid material can be performed by F$^-$-catalyzed hydrolysis under different experimental conditions that change the nucleophilic power of F$^-$. The present results demonstrate the great influence of this nucleophilic power, which controls the three chemical transformations promoted by F$^-$, occurring during the chemical treatment: cleavage of the Si—C$_{sp}$ bond, polycondensation of the Si—OR (R = H or CH$_3$) units and Si—O—Si redistribution. These reactions are known to proceed in solution, their concurrent occurrence here is the key of the morphology of the residues. The dramatic modifications that result can suppress the organization of the organic spacers in the hybrid xerogel. This points out the limitation of the use of silica-based materials for molecular imprinting.[21,2,25] Alternatively, this approach could provide a route to silica with adjustable porosity.

Experimental

Instrumentation

^{1}H and ^{13}C NMR spectra were recorded on a Bruker DPX200, ^{1}H at 200 MHz and ^{13}C at 50.323 MHz. Chemical shifts are reported in ppm relative to either TMS (0.00 ppm) or CDCl$_3$ (7.29 ppm) as internal standards. Abbreviations are as follows: s, singlet; d, doublet; t, triplet; q, quartet; m, multiplet and refer to the appropriate coupling. ^{29}Si NMR in solid state NMR spectra were obtained on a AM300 at 59.620 MHz. Elemental analyses were performed by the "Service de Microanalyse du CNRS". Infrared spectra were recorded in KBr pellets on a Perkin Elmer 1600 FTIR spectrophotometer. Surface area measurements were conducted on a Micromeritics Gemini porosimeter using high purity N$_2$ as adsorbate at 77 K. Surface areas were calculated by the BET equation and pore distributions characterized by the BJH method. Thermogravimetric analyses were performed on a Netzsch STA 409 thermobalance under a 50 mL min^{-1} air flow. Samples were heated from 20–1000 °C at 10 °C min^{-1}. Helium pycnometry measurements were performed on a Accupyc1330 pycnometer. Samples were dried under vacuum at 100 °C for 12 h before analysis. SAXS experiments were carried out on a high resolution Bonse-Hart camera with two germanium channel cuts for very small q values (three reflections on 111 planes for each crystal) and on a low resolution classical apparatus with a Ge(111) monochromator and a linear detector for q values >0.03 Å^{-1}. The wavelength is 1.542 Å (CuKα radiation). The specimens were powdered and dried samples.

General procedures

All reactions were carried out under nitrogen by use of a vacuum line and Schlenk tube techniques. THF was dried on

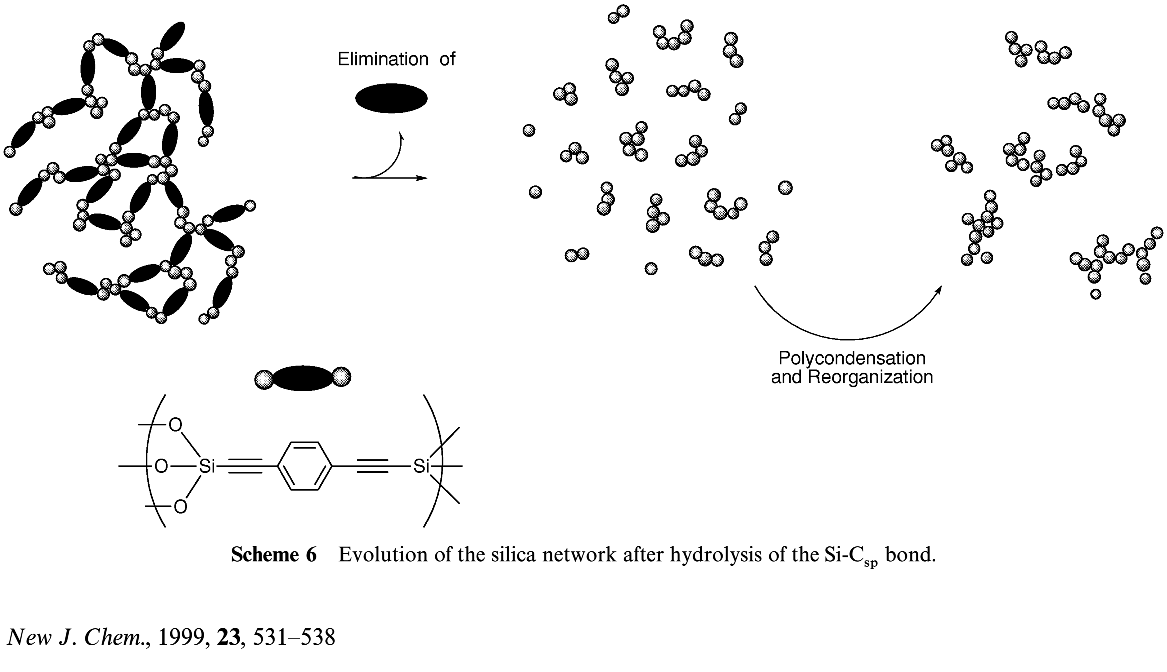

Scheme 6 Evolution of the silica network after hydrolysis of the Si-C$_{sp}$ bond.

Na and distilled under nitrogen using standard procedures.[43] 1,4-Bis(trimethoxysilylethynyl)benzene was synthesized as described by Chevalier *et al.*[21]

Preparation of H_1. Polycondensation of 1,4-bis(trimethoxysilylethynyl)benzene. The monomer (15.54 g, 42.0 mmol) was dissolved in THF (14.2 mL) in a Schlenk flask. Then deionized water (pH = 6, 2.3 mL, 126.0 mmol) was added while stirring the clear and homogeneous solution. Gelation occurred within 5 min. The gel was aged for 1 week at room temperature in the dark, then crushed, washed with ethyl ether and finally dried under vacuum at 100 °C to give 10.34 g of a yellowish powder. ^{13}C NMR (solid state) CP-TOSS δ: 50.6, 89.9, 102.5, 123.1, 132.3. ^{29}Si NMR CP MAS δ: −78.8 (T^1), −87.2 (T^2), −96.6 (T^3). Anal. calcd for $C_{10}H_4O_3Si_2$: C, 52.61; H, 1.77; O, 21.02; Si, 24.60; found: C, 49.96; H, 4.04; O, 23.70; Si, 21.70. IR (KBr): 1066, 1499, 2172, 2878, 2977, 3425 cm^{-1}. TGA: onset 20 °C, end 300 °C, loss of 9.3%; onset 300 °C; end 700 °C, loss of 43.3%; no loss above 900 °C.

Chemical treatment. In a typical experiment, chemical treatment of the xerogel was performed in a 50 mL one-neck flask with reflux condenser and magnetic stirrer. The reagents, solvent (10.5 mL), H_2O (21 mL) and aqueous 1 M catalyst solution (0.2 mL, 0.2 mmol) were added and the suspension was heated at 60 °C for 4 days with gentle stirring. The solution was then filtered, the solid washed with H_2O, THF, acetone, ether and dried for 24 h at room temperature.

Preparation of C_1. Xerogel H_1 (2.00 g, 8.8 mmol calculated for a molecular weight where all the methoxy functions are condensed) and reagents (THF as solvent and NH_4F as catalyst) were mixed and reacted. After removal of the solvent, 0.691 g of an orange powder was recovered. ^{29}Si NMR CP MAS δ: −61.26, −91.31 (Q^2), −100.82 (Q^3), −110.52 (Q^4). FTIR (KBr): 804.2, 967.6, 1142.0, 1501.6, 3455.1 cm^{-1}. TGA: onset 20 °C, end 250 °C, loss of 4.9%; onset 250 °C, end 800 °C, loss of 39.9%.

Preparation of C_2. Xerogel H_1 (2.00 g, 8.8 mmol calculated for a molecular weight where all the methoxy functions are condensed) and reagents (ethanol as solvent and NH_4F as catalyst) were mixed and reacted. After removal of the solvent, 1.027 g of a yellowish powder was recovered. ^{29}Si NMR CP MAS δ: −90.61 (Q^2), −99.77 (Q^3), −111.34 (Q^4). FTIR (KBr): 798.7, 967.6, 1152.9, 3433.3 cm^{-1}. TGA: onset 20 °C, end 280 °C, loss of 2.7%; onset 280 °C, end 800 °C, loss of 3.3%.

Preparation of C_3. Xerogel H_1 (2.00 g, 8.8 mmol calculated for a molecular weight where all the methoxy functions are condensed) and reagents (methanol as solvent and NBu_4F as catalyst) were mixed and reacted. After removal of the solvent, 0.933 g of a white powder was recovered. ^{29}Si NMR CP MAS δ: −101.95 (Q^3), −110.95 (Q^4). FTIR (KBr): 798.7, 973.1, 1098.4, 1229.2, 3487.8 cm^{-1}. TGA: onset 20 °C, end 250 °C, loss of 2.2%; onset 250 °C, end 720 °C, loss of 3.3%.

Preparation of C_4. Xerogel H_1 (2.00 g, 8.8 mmol calculated for a molecular weight where all the methoxy functions are condensed) and reagents (methanol as solvent and NH_4F as catalyst, pH of the water solution was adjusted to 3 with HCl before addition, the pH of the reaction mixture was 4.0) were mixed and reacted. After removal of the solvent, 0.889 g of a white powder was recovered. ^{29}Si NMR CP MAS δ: −91.39 (Q^2), −100.26 (Q^3), −110.59 (Q^4) FTIR (KBr): 793.3, 967.6, 1109.3, 3487.8 cm^{-1}. TGA: onset 20 °C, end 220 °C, loss of 3.3%; onset 220 °C, end 675 °C, loss of 4.4%.

Preparation of C_5. Xerogel H_1 (2.00 g, 8.8 mmol calculated for a molecular weight where all the methoxy functions are condensed) and reagents (methanol as solvent and NH_4F as catalyst, pH of the water solution was adjusted to 10 with NaOH, the pH of the reaction mixture was 7.7) were mixed and reacted. After removal of the solvent, 0.968 g of a white powder was recovered. ^{29}Si NMR CP MAS δ: −100.38 (Q^3), −111.08 (Q^4). FTIR (KBr): 798.7, 973.1, 1087.5, 1229.2, 3487.8 cm^{-1}. TGA: onset 20 °C, end 270 °C, loss of 0.9%; onset 270 °C, end 800 °C, loss of 4.3%.

Preparation of C_6. Xerogel H_1 (2.00 g, 8.8 mmol calculated for a molecular weight where all the methoxy functions are condensed) and reagents (methanol as solvent and NH_4F as catalyst) were mixed and reacted. After removal of the solvent, 0.968 g of a white powder was recovered. ^{29}Si NMR CP MAS δ: −90.70 (Q^2), −100.40 (Q^3), −110.80 (Q^4). FTIR (KBr): 973.1, 1080.0, 2889.0, 2987.0, 3436.0 cm^{-1}. TGA: onset 20 °C, end 250 °C, loss of 6.3%; onset 250 °C, end 1000 °C, loss of 5.7%.

References

1 F. H. Dickey, *Proc. Natl. Acad. Sci. USA*, 1949, **35**, 227.
2 G. Wulff, *Angew. Chem., Int. Ed. Engl.*, 1995, **34**, 1812.
3 S. Dai, Y. S. Shin, C. E. Barnes and L. M. Toth, *Chem. Mater.*, 1997, **9**, 2521.
4 C. Pinel, P. Loisil and P. Gallezot, *Adv. Mater.*, 1997, **9**, 582.
5 M. Tsionsky, A. Vanger and O. Lev., *Sol-Gel Sci. Technol.*, 1994, **2**, 595.
6 C. J. Brinker, R. Sehgal, S. L. Hietal, R. Despande, M. M. Smith, D. Loy and C. S. Ashley, *J. Membrane Sci.*, 1994, **94**, 85.
7 K. N. Raman, M. T. Anderson and C. J. Brinker, *Chem. Mater.*, 1996, **8**, 1682.
8 Y. Chujo, S. Matsuki, T. Kure, T. Saegusu and T. Yazawa, *J. Chem. Soc., Chem. Commun.*, 1994, 635.
9 M. Antonietti, B. Berton, C. Goltner and H. P. Hentze, *Adv. Mater.*, 1998, **10**, 155.
10 C. T. Kresge, M. E. Leonowicz, W. J. Roth, J. C. Vartuli and J. S. Beck, *Nature* (*London*), 1992, **710**, 359.
11 C. T. Kresge, M. E. Leonowicz, W. J. Roth, J. C. Vartuli, J. S. Beck, K. D. Schimtt, C. T. Chu, K. H. Olson, E. Sheppard, S. B. McCullen, J. B. Higgins and J. L. Schlenker, *J. Am. Chem. Soc.*, 1992, **114**, 10834.
12 G. S. Attard, J. C. Glyde and C. G. Goeltner, *Nature* (*London*), 1995, **378**, 366.
13 R. Makote and M. M. Collinson, *Chem. Mater.*, 1998, **10**, 2440.
14 Y. Wei, D. Jin, T. Ding, W. H. Shih, X. Liu, S. Z. D. Cheng and Q. Fu, *Adv. Mater.*, 1998, **3**, 313.
15 U. Schubert, N. Hüsing and A. Lorenz, *Chem. Mater.*, 1995, **7**, 2010.
16 C. Sanchez and F. Ribot, *New J. Chem.*, 1994, **18**, 1007.
17 D. A. Loy and K. J. Shea, *Chem. Rev.*, 1995, **95**, 1431.
18 R. J. P. Corriu and D. Leclercq, *Angew. Chem., Int. Ed. Engl.*, 1996, **35**, 1422.
19 G. Cerveau and R. J. P. Corriu, *Coord. Chem. Rev.*, 1998, **180**, 1051.
20 R. J. P. Corriu, J. J. E. Moreau, P. Thèpot and M. Wong Chi Man, *Chem. Mater.*, 1992, **4**, 1217.
21 P. Chevalier, R. J. P. Corriu, P. Delord, J. J. E. Moreau and M. Wong Chi Man, *New J. Chem.*, 1998, **22**, 423.
22 P. Chevalier, R. J. P. Corriu, J. J. Moreau and M. Wong Chi Man, *Sol-Gel Sci. Technol.*, 1997, **8**, 603.

23 B. Boury, P. Chevalier, R. J. P. Corriu, P. Delord, J. J. E. Moreau and M. Wong Chi Man, *Chem. Mater.*, 1999, **11**, 281.

24 P. Chevalier, Ph.D. Thesis, Université Montpellier II, 1995.

25 R. J. P. Corriu, J. J. E. Moreau, P. Thépot and M. Wong Chi Man, *Chem. Mater.*, 1996, **100**, 8.

26 R. J. P Corriu, R. Perz and C. Réye, *Tetrahedron*, 1983, **39**, 999.

27 A. Bassindale and P. G. Taylor, in *The Chemistry of Organosilicon Compounds*, eds. S. Patai and Z. Rappaport, John Wiley and Son, New York, 1989, Part 2, ch. 14, p. 893.

28 R. J. P. Corriu, G. Dabosi and M. Martineau, *J. Organomet. Chem.*, 1978, **150**, 27.

29 R. J. P. Corriu, G. Dabosi and M. Martineau, *J. Organomet. Chem.*, 1978, **154**, 33.

30 R. J. P. Corriu, G. Dabosi and M. Martineau, *J. Organomet. Chem.*, 1980, **186**, 25.

31 R. J. P. Corriu, C. Guerin and J. J. E. Moreau, *Top Curr. Chem.*, 1984, **15**, 43.

32 I. Kuwajima, E. Nakamura and K. Hashimoto, *Tetrahedron*, 1983, **39**, 975.

33 C. Chuit, R. J. P. Corriu, C. Reyé and C. Young, *Chem. Rev.*, 1993, **93**, 1371.

34 C. Chuit, R. J. P. Corriu, and C. Réye, *J. Organomet. Chem.*, 1988, **358**, 57.

35 K. J. Shea, D. A. Loy and O. Webster, *J. Am. Chem. Soc.*, 1992, **114**, 6700.

36 S. J. Gregg and K. S. W. Sing, *Adsorption Surface Area and Porosity*, Academic Press, London, 1982.

37 S. Lowell and J. E. Shields, *Powder Surface Area and Porosity*, Chapman and Hall, London, 1984.

38 E. P. Barrett, L. Joyner and P. P. Halenda, *J. Am. Chem. Soc.*, 1951, **73**, 373.

39 A. Guinier and G. Fournet, *Small Angle Scattering of X-rays*, John Wiley, New York, 1955.

40 G. Porod, *Small Angle X-ray Scattering*, Academic Press, London, 1982.

41 A. Emmerling and J. Fricke, *J. Non-Cryst. Solids*, 1992, **145**, 113.

42 C. J. Brinker and G. W. Sherer, *Sol-Gel Science*, Academic Press, Boston, 1990.

43 A. Gordon and A. Ford, *Chemist's Companion*, John Wiley & Sons, New York, 1972.

Paper 8/09996K